Diabetologia (2009) 52:2621–2632
DOI 10.1007/s00125-009-1551-0

ARTICLE

Endosomal proteolysis of internalised [Arg^{A0}]-human insulin at neutral pH generates the mature insulin peptide in rat liver in vivo

M. Kouach · B. Desbuquois · F. Authier

Received: 13 July 2009 / Accepted: 8 September 2009 / Published online: 16 October 2009

Abstract
Aims/hypothesis A proteolysis study of human monoarginyl-insulin ([Arg^{A0}]-HI) and diarginyl-insulin ([Arg^{B31}-Arg^{B32}]-HI) within hepatic endosomes was undertaken to determine whether the endosomal compartment represents a physiological site for the removal of Arg residues and conversion of Arg-extended insulins into fully processed human insulin.
Methods The metabolic fate of arginyl-insulins has been studied using the in situ rat liver model system following ligand administration to rats and cell-free hepatic endosomes.
Results While the kinetics of insulin receptor endocytosis after the administration of arginyl-insulins were similar to those observed using human insulin, a more prolonged concentration of endosomal insulin receptor was observed in response to [Arg^{A0}]-HI. [Arg^{A0}]-HI induced a marked increase in the phosphotyrosine content of endosomal insulin receptor, coinciding with a more sustained endosomal association of growth factor receptor-bound protein 14 (GRB14), and a higher and prolonged activation of mitogen-activated protein kinase pathways. At acidic pH, the endosomal cathepsin D rapidly degraded insulin peptides with similar binding affinity, and generated comparable intermediates for both arginyl-insulins without affecting amino and carboxyl arginyl-peptide bonds. At neutral pH, hepatic endosomes fully processed [Arg^{A0}]-HI into mature human insulin while no conversion was observed with [Arg^{B31}-Arg^{B32}]-HI. The neutral endosomal Arg-convertase was sensitive to bestatin, immunologically distinct from insulin-degrading enzyme, nardilysin or furin, and was potentially related to aminopeptidase-B-type enzyme.
Conclusions/interpretation The data describe a unique processing pathway for the endosomal proteolysis of [Arg^{A0}]-HI which involves the removal of Arg^{A0} and subsequent generation of mature human insulin through an uncovered neutral Arg-aminopeptidase activity. The endosomal conversion of [Arg^{A0}]-HI into human insulin might extend the insulin receptor signalling at this locus.

Keywords Cathepsin · Endocytosis · Endosome · Hepatocyte · Insulin · Liver · Protease

Abbreviations

[Arg^{A0}]-HI	Human monoarginyl-insulin
[Arg^{B31}-Arg^{B32}]-HI	Human diarginyl-insulin
AP-B	Aminopeptidase B
CD	Cathepsin D
EN	Endosomal fraction
ENs	Soluble endosomal extract
GRB14	Growth factor receptor-bound protein 14

M. Kouach
Faculté de Pharmacie,
Centre Universitaire de Mesures et d'Analyses (CUMA),
Lille, France

B. Desbuquois
INSERM U567,
Paris, France

B. Desbuquois
Institut Cochin, Université Paris Descartes, CNRS (UMR 8104),
Paris, France

F. Authier (✉)
INSERM U756, Faculté de Pharmacie,
5 rue Jean-Baptiste Clément,
92296 Châtenay-Malabry, France
e-mail: francois.authier@u-psud.fr

F. Authier
Faculté de Pharmacie, Université Paris-Sud,
Châtenay-Malabry, France

HI	Human insulin
HPI	Human proinsulin
IDE	Insulin-degrading enzyme
IR	Insulin receptor
MAP	Mitogen-activated protein
PY	Phosphotyrosine
RP-HPLC	Reverse-phase HPLC
SHC	SHC adaptor protein

Introduction

Endoproteolytic cleavage of protein prohormones often generates intermediates extended at the C-terminus by Arg-Arg or Lys-Arg, the removal of which by carboxypeptidases is an important step in the complete maturation of polypeptide hormones. In the secretory granules of pancreatic beta cells, conversion of proinsulin to insulin occurs with the removal of the C-peptide connecting the C-terminus of insulin B-chain to the N-terminus of the insulin A-chain [1]. The conversion of proinsulin to insulin involves endoproteolytic cleavages on the carboxyl side of the basic Arg^{31}-Arg^{32} and Lys^{64}-Arg^{65} bonds by the proprotein convertases PC3 and PC2; the remaining C-terminal Arg residues are then removed by carboxypeptidase H [2]. During the conversion of proinsulin and the subsequent release of mature insulin, C-peptide and free Arg and Lys into the blood circulation, incompletely cleaved intermediates (des-[64,65]- and des-[31,32]-proinsulins, mono- and diarginyl-insulins) as well as intact proinsulin were concomitantly released in plasma with levels being possibly increased under pathological states conditions [3].

It has been proposed that proinsulin, which is normally processed in secretory granules and released via the regulated pathway, may also be processed—albeit less efficiently—by target tissue (hepatic parenchyma) [4–6]. Thus, rat liver endosomal extracts have been shown to process proinsulin within the C-peptide region at the dibasic motifs 31-32 and 64-65 [4–6]. Comparably, rat hepatoma Fao cells stably transfected with proinsulin have been shown to process proinsulin intracellularly, generating split forms of proinsulin as well as fully processed insulin [5].

Human diarginyl-insulin ([Arg^{B31}-Arg^{B32}]-HI) is one of the major proinsulin intermediates and differs from native insulin by two remaining Arg at the C-terminus of the B-chain [7, 8]. [Arg^{B31}-Arg^{B32}]-HI has almost identical insulin receptor (IR) binding characteristics and full biological activity in vitro as compared with mature human insulin (HI) [7]. Human monoarginyl-insulin ([Arg^{A0}]-HI), another potential arginyl-insulin intermediate, contains an additional Arg at the N-terminus insulin A-chain and displays approximately two-thirds of the binding and biological activity of HI [9, 10]. The reduced biological activity of [Arg^{A0}]-HI can be attributed, at least in part, to modifications in the charge surface and changes in the relative orientation of the two helices in the A-chain [11, 12].

The question then arises as to whether the endosomal compartment of hepatic target tissue should be considered as an alternative processing site for the removal of basic residues from internalised Arg-extended peptides. Consequently, the present study has attempted to evaluate the physiological relevance of hepatic endosomes for the conversion of mono- and diarginyl-insulins into mature insulin. Reverse phase-HPLC (RP-HPLC) and mass spectrometry analyses revealed that production of mature insulin occurs at pH 7 during incubation of [Arg^{A0}]-HI with hepatic endosomes, while no conversion was observed using [Arg^{B31}-Arg^{B32}]-HI under these same conditions. Using immunological criteria and the Arg-MCA fluorescence assay, we show also that the neutral proteolytic activity which removes the single N-terminal Arg in [Arg^{A0}]-HI is a bestatin-sensitive aminopeptidase activity that is possibly related to aminopeptidase-B (AP-B) [13]. Finally, while both arginyl-insulins induced the endocytosis and tyrosine phosphorylation of the IR in vivo, only the [Arg^{A0}]-HI treatment resulted in a higher extent and duration of IR tyrosine phosphorylation and a prolonged residence time of IR at the endosomal locus.

Methods

Peptides, antibodies, protein determination and materials HI [Arg^{A0}]-HI and *Z*-L-Arg 7-amido-4-methylcoumarine hydrochloride (Arg-MCA) were purchased from Sigma (St Louis, MO, USA). [Arg^{B31}-Arg^{B32}]-HI was supplied by Eli Lilly (Indianapolis, IN, USA) and obtained from R. E. Isaac (University of Leeds, Leeds, UK). HI was radioiodinated as described previously [14]. Polyclonal antibody to SHC-adaptor protein (SHC) was obtained from J. J. M. Bergeron (McGill University, Montreal, Canada). Polyclonal IgG preparations against the human IR-β subunit and rat insulin receptor substrate-1 (IRS-1), and monoclonal anti-phosphotyrosine (PY) (clone 4G10) were purchased from UBI (Lake Placid, NY, USA). Monoclonal IgG against AP-B (clone 4E1) was from Sigma. Polyclonal IgG against human phospho-p44/42 mitogen-activated protein (MAP) kinase and rat p44/42 MAP kinase proteins were from Cell Signaling Technology (Danvers, MA, USA). Polyclonal antibody against growth factor receptor-bound protein 14 (GRB14) has been previously described [15]. Rabbit anti-mouse cathepsin D R291 [16, 17], sheep anti-human cathepsin D M8147 [16, 17] and rabbit anti-rat cathepsin B 7183 [18] were obtained from J. S. Mort (Shriners Hospital for Crippled Children, Montreal, Canada). Monoclonal antibody directed against insulin-degrading enzyme

(IDE) [19, 20] was obtained from R. A. Roth (Stanford University, Stanford, CA, USA). Polyclonal antibody to nardilysin was obtained from L. B. Hersh (University of Kentucky, Lexington, KY, USA). Polyclonal antibody against human furin was from Santa Cruz Biotechnology (Santa Cruz, CA, USA) [21, 22]. The protein content was determined by the method of Lowry et al. [23]. All other chemicals were obtained from commercial sources and were of reagent grade.

Animals

In vivo procedures were approved by the Institutional Committee for the Use and Care of Experimental Animals. Male Sprague–Dawley rats, body weight 180–200 g, were obtained from Charles River France (St Aubin Les Elbeufs, France) and fasted for 18 h prior to sacrifice. Native insulin peptides (15 μg/100 g body weight) in 0.4 ml of 0.15 mol/l NaCl was injected within 5 s into the penile vein under light anaesthesia with ether.

Rat liver subcellular fractionation Subcellular fractionation was performed using established procedures as previously described. Nuclear, mitochondrial lysosomal, microsomal and cytosolic fractions were isolated by differential centrifugation [14, 16–19, 21, 22, 24, 25]. The endosomal fraction (EN) was isolated by discontinuous sucrose gradient centrifugation and collected at the 0.25–1.0 mol/l sucrose interface [14, 16–19, 21, 22, 24, 25]. Soluble endosomal extract (ENs) was isolated from the EN fraction as previously described [14, 16–19, 21, 22, 24, 25].

Immunoblot analysis Electrophoresed samples were transferred as described previously [16–22] and the membranes were then incubated with primary antibody (antibodies against SHC diluted 1:5000, IR-β subunit diluted 1:1000, phospho-p44/42 MAP kinase diluted 1:350, p44/42 MAP kinase diluted 1:350, GRB14 diluted 1:500, IRS-1 diluted 1:1000, nardilysin diluted 1:1000, PY diluted 1:2500 or AP-B diluted 1:200). The bound immunoglobulin was detected using horseradish peroxidase-conjugated goat anti-rabbit or anti-mouse IgG. Quantification of protein signals were done by scanning densitometry using the analysis program Scion Image (Frederick, MA, USA).

Immunodepletion studies ENs was immunodepleted of endosomal proteases prior to the digestion step by incubating ENs (0.15 mg/ml) with antibodies coated onto protein G-Sepharose beads for 16 h at 4°C in 800 μl of 20 mmol/l sodium phosphate buffer (pH 7). The fractions were then centrifuged for 5 min at 10,000×*g*, and the resultant immunodepleted supernatant fractions were adjusted to pH 4 with citrate-phosphate buffer and used in the insulin-peptide degradation assay and then immediately assayed by RP-HPLC.

In vitro proteolysis of insulin peptides by endosomes ENs (~1 μg) or EN (1–15 μg) was incubated for varying lengths of time at 37°C with 10 μg insulin peptides in 19 μl of 25 mmol/l citrate-phosphate buffer pH 4 (ENs) or 25 mmol/l Hepes buffer pH 7 containing 6 mmol/l $CaCl_2$ (EN), in the presence or absence of protease inhibitors. The proteolytic reaction was then stopped by the addition of acetic acid (15%) and immediately loaded onto an RP-HPLC column.

For the in vitro degradation of ^{125}I-labelled-Tyr^{A14}-HI by ENs, the radiolabelled HI (40 fmol) was incubated with ENs (~1 μg) and various concentrations of unlabelled HI, [Arg^{A0}]-HI or [Arg^{B31}-Arg^{B32}]-HI in 0.1 mol/l citrate-phosphate buffer, pH 4, for 10 min at 37°C. The amount of radiolabelled HI-degraded was assayed by precipitation with 2 ml of ice-cold 10% trichloroacetic acid (TCA) for 2 h at 4°C. The samples were then centrifuged at 10,000×*g* for 20 min at 4°C, and the supernatant fractions and pellets evaluated for their radioactive content.

HPLC separation of insulin peptides and mass spectrometry RP-HPLC was performed using a Beckman Coulter (Fullerton, CA, USA) System Gold model 127 as previously described [16–18, 21, 26]. Eluates were monitored online for absorbance at 214 nm with a LC-166 spectrophotometer (Beckman Coulter).

Samples were prepared and analysed using ion spray mass spectrometry and HPLC-electron spray ionisation mass spectrometry coupling as previously described [6, 16, 21, 26, 27].

Arginine-aminopeptidase assay Arg-aminopeptidase activity of isolated endosomes was assayed using Arg-MCA substrate [28]. EN (1.5 mg/ml) was incubated with Arg-MCA (200 μmol/l) in 50 mmol/l Tris–HCl, pH 7.4, containing 0.15 mol/l NaCl. The suspensions were immediately placed in the spectrofluorometer, and fluorescence intensities (365/450 nm excitation/emission) were recorded at 37°C for 1–8 h.

Statistics Data are expressed as mean±SD. Statistical evaluations were performed by Student's *t* test. Differences between data groups were considered statistically significant if $p<0.05$.

Results

In vivo effects of arginyl-insulins on IR trafficking and signalling Following the i. v. injection of a single receptor-saturating dose of insulin peptides, the relative levels of IR

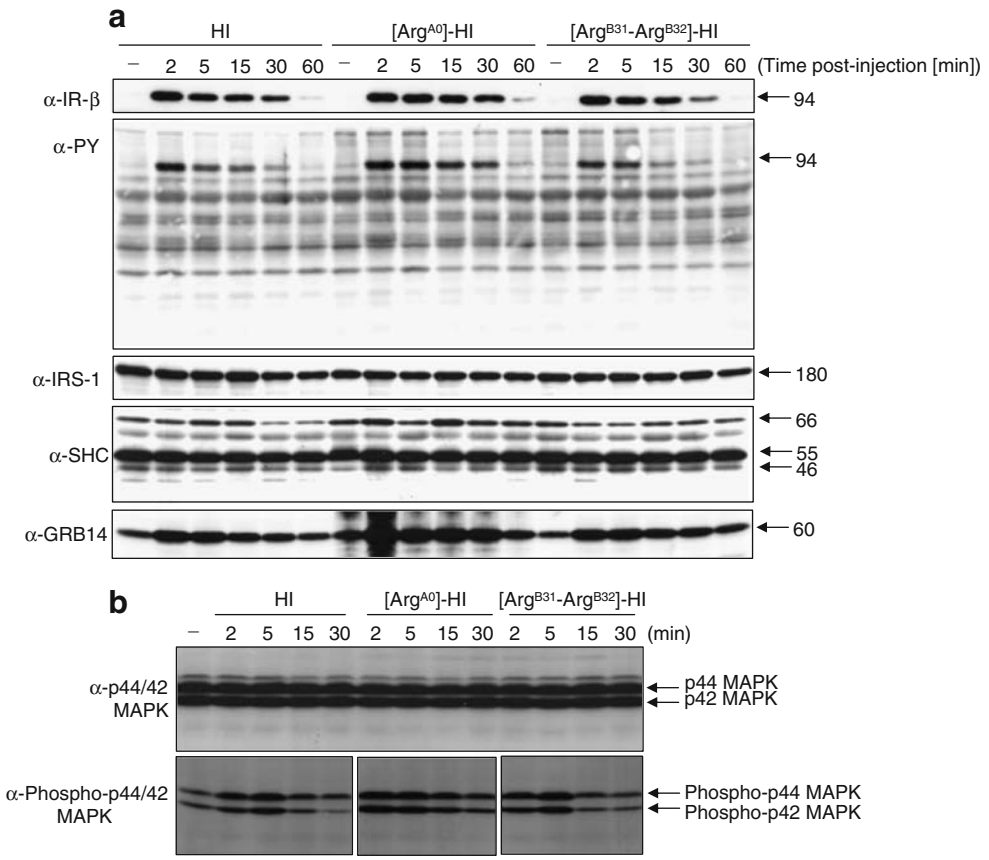

Fig. 1 In vivo effects of HI, [Arg^{A0}]-HI or [Arg^{B31}-Arg^{B32}]-HI on IR-β, IRS-1, SHC, GRB14 and MAP kinase content in hepatic endosomes and cytosol. Endosomes (**a**) or cytosolic fractions (**b**) were isolated at the indicated times after the in vivo administration of native HI, [Arg^{A0}]-HI or [Arg^{B31}-Arg^{B32}]-HI (15 μg/100 g body weight), and evaluated by Western blot analysis for content of IR-β, IRS-1, SHC, GRB14 (endosomes, **a**) and MAP kinase (MAPK; cytosol, **b**), and for their immunoreactivity with antibodies against PY (endosomes, **a**) or phospho-MAP kinase (cytosol, **b**). Each lane contains ~80 μg of endosomal protein or 30 μg of cytosolic protein. Arrows to the right indicate the mobilities of the IR-β subunit (~94 kDa), IRS-1 (~180 kDa), SHC (~66, 55 and 46 kDa) and GRB14 (~60 kDa). Each experiment was reproduced three times and the blots shown are representative of the data. Protein signals were quantified by scanning densitometry and the results expressed as % ± SD signal intensity in [Arg^{A0}]-HI-treated rats in comparison with HI-treated rats. α-IR-β blot: 130±4.6% (5 min, $p<0.01$); 122±7.6% (15 min, $p<0.01$); 153±7.0% (30 min, $p<0.001$). α-PY blot: 125±9.0% (2 min, $p<0.05$); 181±5.5% (5 min, $p<0.01$); 189±8.9% (15 min, $p<0.01$); 224±10.6% (30 min, $p<0.001$). α-GRB14 blot: 147±7.6% (2 min, $p<0.01$); 152±5.8% (5 min, $p<0.01$); 165±5.5% (15 min, $p<0.01$); 178±4.7% (30 min, $p<0.01$)

in rat liver endosomal fractions were measured by immunoblotting with antibody raised to IR-β subunit (Fig. 1a, α-IR-β blot). An increase in IR-β subunit was observed 2 min after administration of either insulin peptides, with both showing identical initial internalisation kinetics (up to 2 min). In response to HI and [Arg^{B31}-Arg^{B32}]-HI, the level attained was maximal at 2 min with a return to background levels observed after 60 min. However, in response to [Arg^{A0}]-HI, an accumulation of IR-β was observed in the EN fractions for up to 5 min before decreasing with time. Tyrosine-phosphorylated IR was detected 2 min after administration of either of the three ligands (Fig. 1a, α-PY blot). A higher and more prolonged PY content was observed for [Arg^{A0}]-HI at 5 min post injection with the level remaining elevated up to 30 min.

To study the effect of arginyl-insulin administration on protein adaptor compartmentalisation, rat-liver-derived EN fractions were assayed for IRS-1, SHC and GRB14 content after ligand injection (Fig. 1a, three lower blots). All three protein adaptors were detected in EN fractions isolated from control rats (lanes –). Administration of HI [24] or arginyl-insulins did not cause detectable changes in the levels of IRS-1 or SHC isoforms at the endosomal locus. In contrast, the three ligands led to a rapid increase in the content of the molecular adaptor GRB14 within EN fractions [15]. Endosomal association of GRB14 was more sustained after the administration of [Arg^{A0}]-HI, which paralleled its effect on phosphorylated IR-β content.

MAP kinase activity was then assayed in response to ligand administration by immunoblotting cytosolic fractions

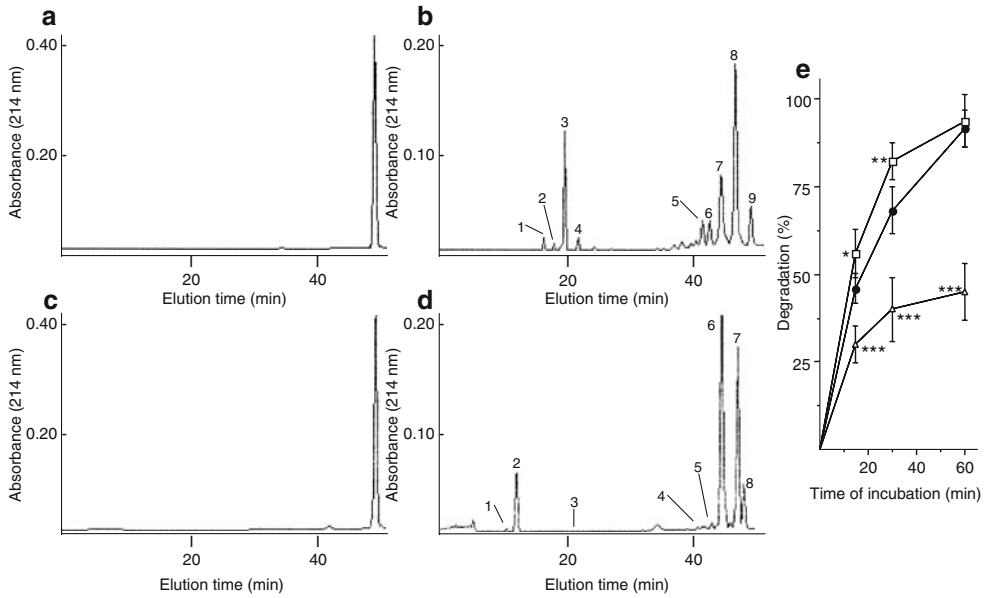

Fig. 2 In vitro proteolysis of native [Arg^{A0}]-HI and [Arg^{B31}-Arg^{B32}]-HI at pH 4 by a soluble endosomal lysate. **a–d** Representative RP-HPLC absorbance profiles at 214 nm resulting from the incubation of native [Arg^{A0}]-HI (**a**, **b**) or [Arg^{B31}-Arg^{B32}]-HI (**c**, **d**), 2 μmol/l, with ENs (~1 μg) at 37°C for 2.5 h in citrate-phosphate buffer, pH 4 (RP-HPLC profiles **b**, **d**). Elution profiles of native [Arg^{A0}]-HI (**a**) and [Arg^{B31}-Arg^{B32}]-HI (**c**) are shown for comparison. Intact [Arg^{A0}]-HI and [Arg^{B31}-Arg^{B32}]-HI had elution times of 49 and 48 min, respectively. The endosomal proteins alone did not give any detectable peaks (results not shown). The major peptide pools, numbered sequentially 1–9, were collected and subjected to mass spectrometry analyses (see Table 1). **e** Kinetics of processing of HI (black circles), [Arg^{A0}]-HI (white squares) and [Arg^{B31}-Arg^{B32}]-HI (white triangles) at pH 4 by a soluble endosomal lysate. The in vitro proteolysis of HI and the two arginyl-insulin peptides was measured by RP-HPLC analysis as described in (**b**) and (**d**) by following the disappearance of the peak area corresponding to the parent peptides. Results are expressed as the percentage of peptide degraded after a 15, 30 or 60 min incubation, and normalised (100%) to that seen in the absence of added endosomal protein. Results are the mean±SD of three different experiments performed on endosomal fractions prepared from separate liver fractionations. *p<0.05, **p<0.01 and ***p< 0.001 for the differences between arginyl-insulins and HI

with antibodies against total or phosphorylated p44/42 MAP kinase proteins (Fig. 1b). MAP kinase activation increased in response to all ligands with a maximal effect at 5 min for HI and [Arg^{B31}-Arg^{B32}]-HI, or 2–5 min for [Arg^{A0}]-HI. By 15 min, p44/42 MAP kinase phosphorylation had returned to background levels in response to HI or [Arg^{B31}-Arg^{B32}]-HI ligand, whereas it remained elevated in response to [Arg^{A0}]-HI.

Catalytic properties of endosomal arginyl-insulin-degrading activity at acidic pH We next examined the ability of a soluble endosomal lysate to proteolyse arginyl-insulins in vitro at acidic pH as compared with native HI (Fig. 2). The rate of hydrolysis of each peptide was determined by following the disappearance of the parent peptide on RP-HPLC (peak 9 for [Arg^{A0}]-HI or peak 8 for [Arg^{B31}-Arg^{B32}]-HI) after a 15, 30 or 60 min incubation with ENs at pH 4 (Fig. 2e). Incubation of HI or [Arg^{A0}]-HI with ENs resulted in a rapid degradation of peptides with 46% and 55% proteolysis, respectively, after a 15 min incubation period. With the [Arg^{B31}-Arg^{B32}]-HI peptide, less than 45% degradation was detected after a 1 h incubation period.

The effect of various protease inhibitors on the acidic arginyl-insulin-degrading activity contained in hepatic endosomes was next examined by RP-HPLC analysis (Fig. 3a,b). The proteolytic activity directed against both arginyl-insulins at pH 4 was inhibited by pepstatin-A, an inhibitor of aspartic acid proteases.

The inhibition of arginyl-insulin-degrading activity by pepstatin-A suggested cathepsin D as a likely candidate for this activity. We therefore used well-characterised antibodies to mature cathepsin D and its proform [16, 17] to deplete cathepsin D from ENs (Fig. 3a,c). Quantitative immunoprecipitation of cathepsin D using antibodies directed against the mouse (R291) and human enzyme (M8147) removed more than 80% of the endosomal proteolytic activity directed towards both arginyl-insulins as assessed by RP-HPLC (Fig. 3a, lower panels, and c). Immunodepletion of ENs with antibodies to either cathepsin B [18], IDE [19, 20], furin [21, 22] or nardilysin failed to remove the arginyl-degrading activity (Fig. 3c).

Substrates of the same protease would be expected to compete with each other for the enzyme binding site. We therefore used a competition assay to evaluate the ability of native arginyl-insulins to inhibit degradation of the radio-

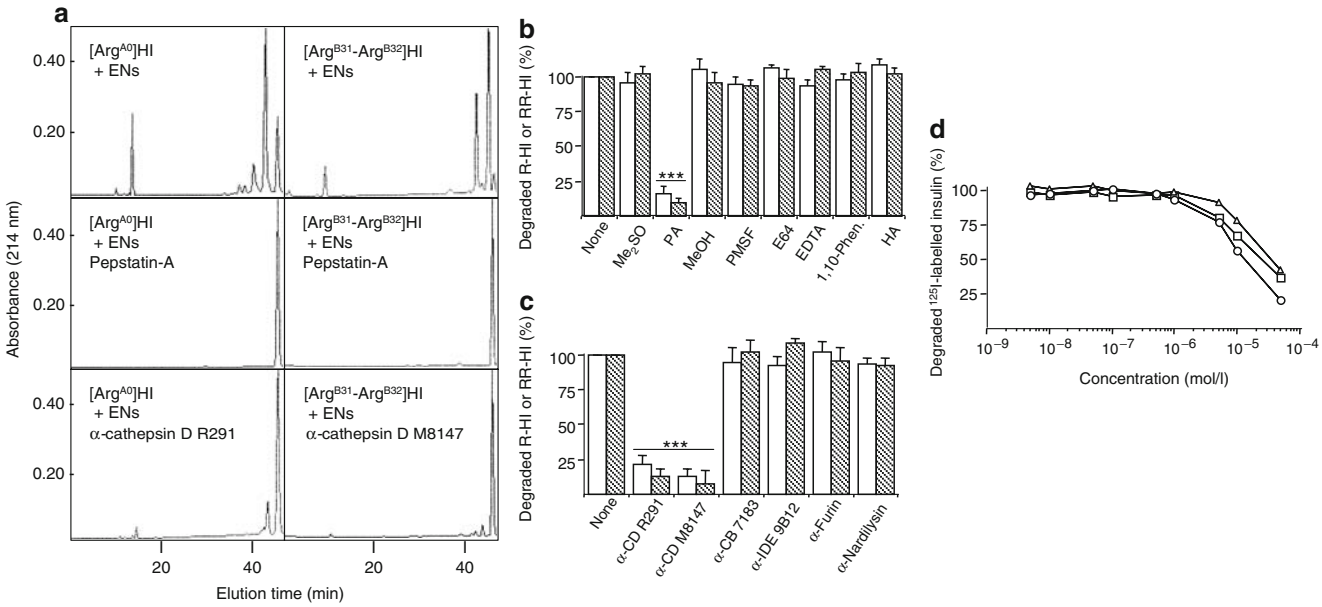

Fig. 3 Effects of protease inhibitors and immunodepletion of cathepsins on the proteolysis of [Arg^{A0}]-HI and [Arg^{B31}-Arg^{B32}]-HI by hepatic endosomes. **a** Representative RP-HPLC profiles obtained following the incubation of [Arg^{A0}]-HI and [Arg^{B31}-Arg^{B32}]-HI at pH 4 with: ENs (upper profiles); ENs in the presence of pepstatin-A (middle profiles); and ENs which had been immunodepleted of active cathepsin D using anti-cathepsin D R291 or anti-cathepsin D M8147 antibody (lower profiles). Absorbance profiles at 214 nm are shown. **b** ENs (~1 μg) was incubated with 2 μmol/l [Arg^{A0}]-HI (white bars) or [Arg^{B31}-Arg^{B32}]-HI (hatched bars) at 37°C for 90 min in citrate-phosphate buffer, pH 4, in the absence of all of the following (none), or the presence of 1% (vol./vol.) DMSO (Me_2SO), 1 μg/ml pepstatin-A (PA), 1% (vol./vol.) MeOH, 1 mmol/l phenylmethylsulfonyl fluoride (PMSF), 1 μmol/l E64, 1 mmol/l EDTA, 1 mmol/l 1,10-phenanthroline (1,10-Phen.) or 1 μmol/l hexa-arginine (HA). At the end of the incubation, the proteolytic reaction was stopped with acetic acid (15% [vol./vol.]), and the incubation mixtures were analysed by RP-HPLC. The rate of proteolysis of [Arg^{A0}]-HI and [Arg^{B31}-Arg^{B32}]-HI was determined by following the disappearance of the peak area corresponding to the parent peptides. The results are expressed as percentage of peptide degraded and normalised to that seen in the absence of added compound. Results are the mean±SD of three different experiments performed on endosomal fractions prepared from separate liver fractionations. ***$p<0.001$ for the difference between pepstatin-A and absence of inhibitors. **c** ENs was immunodepleted of active cathepsin D, cathepsin B, insulin-degrading enzyme, furin or nardilysin using the respective antibodies, and the resultant supernatant fractions were tested for their ability to degrade [Arg^{A0}]-HI (white bars) and [Arg^{B31}-Arg^{B32}]-HI (hatched bars) at pH 4 as described for **b**. Results are the mean±SD of three different experiments performed on endosomal fractions prepared from separate liver fractionations ***$p<0.001$ for the difference between cathepsin-D-immunodepleted and untreated endosomal fractions. **d** Competition of native HI (white squares), [Arg^{A0}]-HI (white triangles) and [Arg^{B31}-Arg^{B32}]-HI (white circles) for the degradation of ^{125}I-labelled Tyr^{A14}-HI by ENs. ENs (~0.1 μg) was incubated with radiolabelled HI in citrate-phosphate buffer, pH 4, with the indicated concentrations of unlabelled peptides. The amount of degraded radiolabelled HI was determined by precipitation with TCA. The results are the mean of three to five separate experiments and are expressed as a percentage of degradation observed in the absence of added unlabelled peptides. For clarity of the curve, error bars are not shown

labelled substrate [^{125}I-labelled Tyr^{A14}]-HI by ENs at pH 4 (Fig. 3d). As reported previously [16, 26], HI was found to inhibit ^{125}I-labelled HI proteolysis by ENs in a dose-dependent manner with an IC_{50} of 2×10^{-5} mol/l. Native arginyl-insulins were found to compete for proteolysis of radiolabelled HI in a manner similar to that observed for HI (IC_{50} 3×10^{-5} and 1×10^{-5} mol/l, respectively).

Sites of cleavage of arginyl-insulin intermediates To determine whether cathepsin D is capable of cleaving arginyl-insulins at the same primary sites as those observed with HI [16, 26], each of the major HPLC peaks generated after a 2.5 h incubation at pH 4 (see Fig. 2b,d) was analysed using mass spectrometry (Table 1, Fig. 4).

Four major early intermediate products, which correspond to the truncated insulin molecule with the C-terminal B-chain clipped off at Arg^{B22}-Gly^{B23}, Gly^{B23}-Phe^{B24}, Phe^{B24}-Phe^{B25} or Phe^{B25}-Tyr^{B26} peptide bonds, were generated from [Arg^{A0}]-HI (products 7b, 7a, 8a and 9b, respectively) or [Arg^{B31}-Arg^{B32}]-HI (products 6a, 7b, 7a and 8b, respectively). Using [Arg^{A0}]-HI as a substrate, two intermediate products corresponding to peptide 7a with the Glu^{B13} or Glu^{B13}-Ala^{B14} missing were referred to as products 9c and 9d, respectively. The production of these primary intermediates correlated with the generation of the C-terminal B-chain endproducts, i.e. Phe^{B25}-Thr^{B30} (product 3), Tyr^{B26}-Thr^{B30} (product 2) and Thr^{B27}-Thr^{B30} (product 1) using [Arg^{A0}]-HI as a substrate, or Phe^{B25}-Arg^{B32} (product 2a), Tyr^{B26}-Arg^{B32} (product 2b) and Thr^{B27}-Arg^{B32} (product 1) using [Arg^{B31}-Arg^{B32}]-HI as a substrate. A mixture of products containing the amino end of the A-chain (Arg^{A0}-Gln^{A15}, Arg^{A0}-Leu^{A16} and Arg^{A0}-Glu^{A17} using [Arg^{A0}]-HI, or Gly^{A1}-Leu^{A13},

Table 1 Masses and assigned structures of the cleavage products generated from native [Arg^{A0}]-HI and [Arg^{B31}-Arg^{B32}]-HI by endosomal acidic insulinase activity

HPLC pools	Retention time (min)	Theoretical calculation (Da)	Mass analysis (amu)
[Arg^{A0}]-HI			
1	16	445.5	445
2	18	608.7	608
3	20	755.8	755
4a	22	1,760.9	1,760
4b	22	1,632.8	1,632
4c	22	1,519.6	1,519
4d	22	1,390.5	1,390
4e	22	1,275.5	1,276
5	41	3,524	3,524
6	42	3,595.1	3,595
7a	44	5,078.8	5,079
7b	44	5,021.7	5,022
7c	44	3,629.1	3,629
7d	44	3,465.9	3,465
7e	44	3,394.9	3,395
8a	47	5,226	5,226
8b	47	3,871.4	3,871
8c	47	3,742.3	3,742
9a	49	5,963.8	5,963
9b	49	5,373.1	5,373
9c	49	4,967.7	4,967
9d	49	4,896.6	4,896
[Arg^{B31}-Arg^{B32}]-HI			
1	10	757.9	757.2
2a	12	1,068.2	1,067.5
2b	12	921.1	920.5
3a	21	1,519.6	1,518.5
3b	21	1,390.5	1,389.5
3c	21	1,275.5	1,276.4
4	41	3,367.8	3,367
5	42	3,481.9	3,481
6a	44	4,865.5	4,865
6b	44	3,309.8	3,308
6c	44	3,238.7	3,237
6d	44	3,196.6	3,195
6e	44	3,125.6	3,124
6f	44	3,068.5	3,067
6g	44	2,997.4	2,996
6h	44	2,905.3	2,904
6i	44	2,834.2	2,833
7a	47	5,069.8	5,068
7b	47	4,922.6	4,922
7c	47	3,553	3,552
7d	47	3,438.9	3,438
8a	48	6,120	6,120
8b	48	5,216.9	5,215

Selected RP-HPLC pools (see HPLC profiles in Fig. 2b,d) generated by endosomal acidic insulinase activity were analysed by RP-HPLC coupled with electron spray ionisation mass spectrometry. Average molecular masses were used for calculations. HPLC pools 4, 7, 8 and 9 generated from [Arg^{A0}]-HI, and 2, 3, 6, 7 and 8 generated from [Arg^{B31}-Arg^{B32}]-HI are heterogeneous. Peptides 9a and 8a are intact [Arg^{A0}]-HI and [Arg^{B31}-Arg^{B32}]-HI, respectively

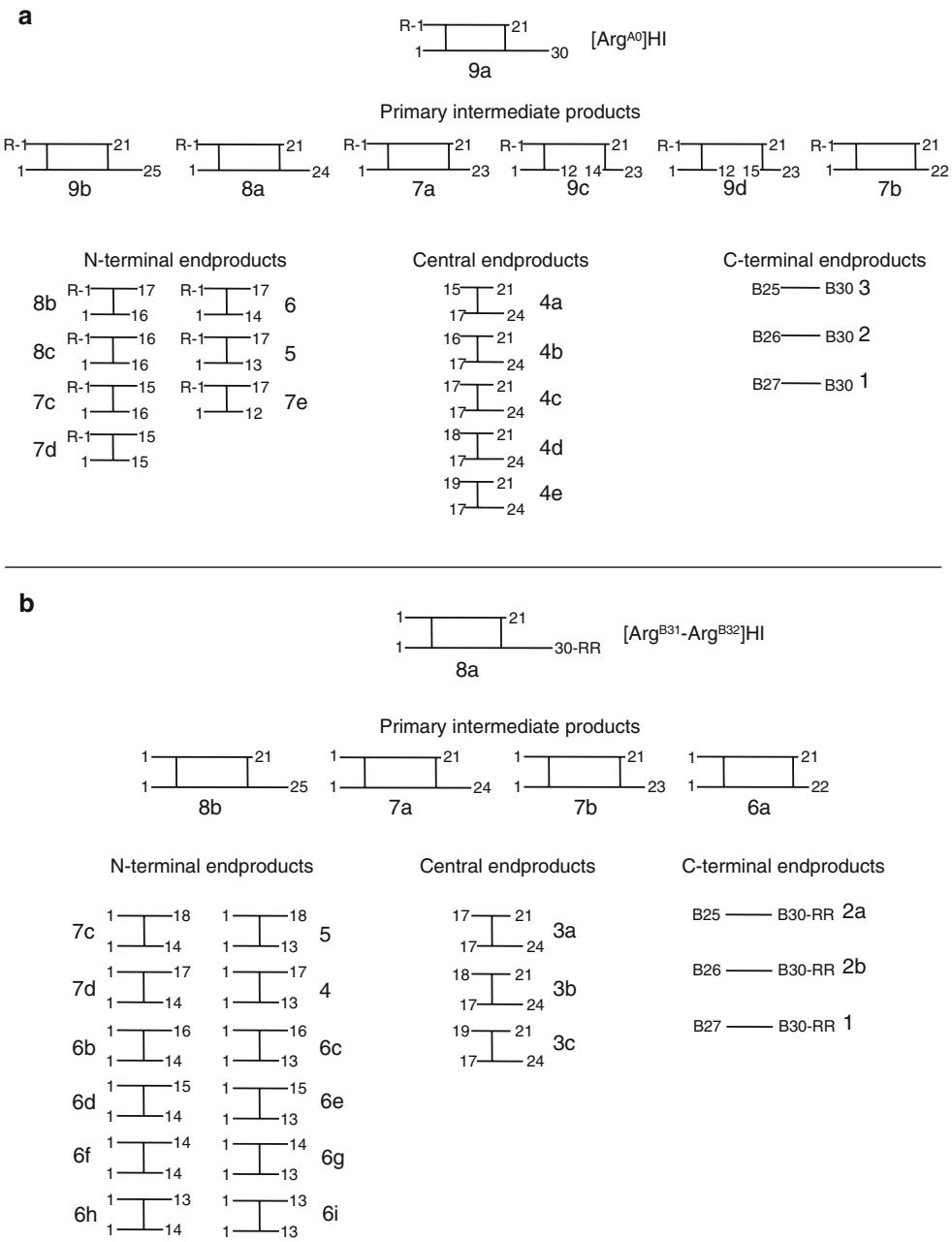

Fig. 4 Structures of intermediates and terminal products generated from [Arg^{A0}]-HI and [Arg^{B31}-Arg^{B32}]-HI by an endosomal lysate at acidic pH. The numbers refer to the degradation products as identified in Fig. 2b, d

Gly^{A1}-Tyr^{A14}, Gly^{A1}-Gln^{A15}, Gly^{A1}-Leu^{A16}, Gly^{A1}-Glu^{A17} and Gly^{A1}-Asn^{A18} using [Arg^{B31}-Arg^{B32}]-HI) connected to the carboxyl end of the B-chain (B$^{1–12}$ to B$^{1–16}$ using [Arg^{A0}]-HI, or B$^{1–13}$ and B$^{1–14}$ using [Arg^{B31}-Arg^{B32}]-HI) were also identified. Finally, a mixture of the remaining C-terminal A-chain (A$^{15–21}$ to A$^{19–21}$) connected to the Leu^{B17}-Phe^{B24} peptide was observed using [Arg^{A0}]-HI (product 4) as a substrate, or A$^{17–21}$ to A$^{19–21}$ connected to the Leu^{B17}-Phe^{B24} peptide (product 3) using [Arg^{B31}-Arg^{B32}]-HI as a substrate.

Endosomal production of fully processed HI from [Arg^{A0}]-HI at neutral pH Hepatic endosomes are known to contain neutral peptidases such as IDE [29], furin [21, 22, 30] and neutral glucagonase activity [21]. Therefore, we evaluated the ability of hepatic endosomes to process arginyl-insulins at neutral pH (Fig. 5a, b) using RP-HPLC analyses. While no processing was observed using [Arg^{B31}-Arg^{B32}]-HI (results not shown), a significant rate of [Arg^{A0}]-HI hydrolysis was detected with generation of the mature HI peptide (mass analysis 5,806 Da). The production of HI was strongly inhibited by bestatin, an inhibitor of aminopeptidases, and metal-chelating agents (EDTA and 1,10-phenanthroline).

Nardilysin and aminopeptidase B (AP-B), two neutral arginine-peptidases [21, 31], represent candidate proteases

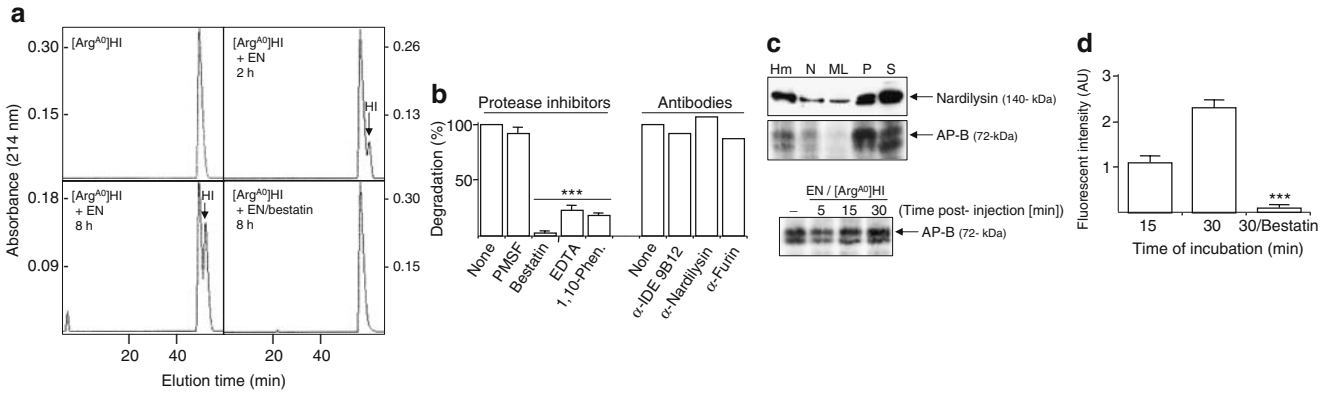

Fig. 5 Processing of [Arg^{A0}]-HI at neutral pH by hepatic endosomes. **a** RP-HPLC profiles of [Arg^{A0}]-HI (2 μmol/l) incubated with EN (~1 μg) at 37°C for different times in Hepes buffer, pH 7, containing 0.15 mol/l NaCl in the absence or presence of 0.1 mmol/l Bestatin. All panels show representative absorbance profiles at 214 nm. **b** For the protease inhibitor assays, EN (~1 μg) was incubated with 2 μmol/l [Arg^{A0}]-HI at 37°C for 5 h in Hepes buffer, pH 7, containing 0.15 mol/l NaCl in the absence of all the following (none), or the presence of: 1 mmol/l phenylmethylsulfonyl fluoride (PMSF), 0.1 mmol/l bestatin, 1 mmol/l EDTA or 1 mmol/l 1,10-phenanthroline (1,10-Phen.). For the antibody assays, supernatant fractions were tested for their ability to degrade [Arg^{A0}]-HI during a 5 h incubation as described for **a**, following immunodepletion, using the respective antibodies, of Triton X-100 solubilised EN of: active insulin-degrading enzyme (α-IDE 9B12), nardilysin (α-nardilysin) and furin (α-furin). Bars labelled 6 show the results with no immunodepletion. At the end of the incubation, the proteolytic reaction was stopped with acetic acid (15% [vol./vol.]) and the incubation mixtures were analysed by RP-HPLC. The rate of proteolysis of [Arg^{A0}]-HI was determined by following the disappearance of the peak area corresponding to the parent peptide. The results are expressed as percentage of peptide degraded and are normalised to that seen in the absence of treatment. The results are the mean±SD of three different experiments (protease inhibitors) or the mean of two different experiments (antibodies) performed on endosomal fractions prepared from separate liver fractionations. ***$p<0.001$ for the difference between bestatin, EDTA or 1,10-phenanthroline and absence of inhibitors. **c** Assessment of nardilysin and aminopeptidase-B (AP-B) by immunoblot analysis of subcellular fractions isolated from rat liver. Nuclear (N), mitochondrial lysosomal (ML), microsomal (P), cytosolic (S) and endosomal (EN) fractions, as well as the isotonic homogenate (Hm) were evaluated by immunoblotting for their content of nardilysin and AP-B. Each lane was loaded with 50 μg protein. EN fractions (lower panel) were isolated from control rats (–) or rats killed at the indicated times after the administration of [Arg^{A0}]-HI. Arrows to the right indicate the mobilities of nardilysin (~140 kDa) and AP-B (~72 kDa). **d** EN fraction isolated from control rats was incubated in 50 mmol/l Tris–HCl, pH 7.4, containing 0.15 mol/l NaCl and 200 μmol/l Arg-MCA in the absence or presence of 0.1 mmol/l bestatin. Fluorescence intensity was immediately measured at 37°C for the indicated times using a recording spectrofluorometer. To monitor the generation of any spontaneous fluorescence, control degradations were performed by incubating the endosomal fractions in the absence of the Arg-MCA synthetic substrate and by incubating the synthetic substrate in the absence of endosomal protein. Both controls gave negligible fluorescent values. Results are expressed as arbitrary units (AU) of fluorescence intensity and are the mean±SD of three determinations performed on EN prepared from separate liver fractionations. ***$p<0.001$ for the difference between 30 min/bestatin and 30 min/untreated

for the production of HI from internalised [Arg^{A0}]-HI. Consequently, we attempted to evaluate the contribution of these proteases to the endosomal degradation of [Arg^{A0}]-HI by immunodepletion of EN (Fig. 5b), or assessment of their content in hepatic endosomes by immunoblot analysis (Fig. 5c). Immunoprecipitation with antibodies to IDE, nardilysin or furin failed to remove the neutral Arg-degrading activity from EN (Fig. 5b). Immunoblot analyses of rat liver homogenate, nuclear, large granule, microsomal and cytosolic fractions from control rats (Fig. 5c, upper blots), and endosomal fractions from non-injected (lane –) or monoarginyl-insulin-injected rats (lanes EN/[Arg^{A0}]-HI) (Fig. 5c, lower blot) revealed that both the cytosolic and microsomal fractions contained the highest concentration of nardilysin and AP-B, suggesting that both proteases displayed a dual soluble and particulate location in rat liver. However, in purified EN, nardilysin was undetectable (results not shown), whereas a small but detectable presence of AP-B was found within hepatic endosomes isolated from control and monoarginyl-insulin-injected rats (Fig. 5c).

We subsequently used Arg-MCA from which a fluorescent product is generated by a single cleavage (Fig. 5d). When EN fractions isolated from control rat livers were incubated at pH 7 with 200 μmol/l Arg-MCA, significant fluorescence intensities were detected after 15 and 30 min of incubation. No hydrolysis of Arg-MCA was detected under conditions of aminopeptidase inhibition (presence of bestatin).

Discussion

We have designed experiments to test whether the Arg residues present in [Arg^{A0}]-HI and [Arg^{B31}-Arg^{B32}]-HI molecules influence IR trafficking during ligand-mediated receptor internalisation and how this affects downstream signalling molecules. Moreover, the endosomal processing

of arginyl-insulins has been studied and compared with that of fully processed HI. Both arginyl-insulins induced the endocytosis and tyrosine phosphorylation of the IR in vivo. However, only the [Arg^{A0}]-HI treatment resulted in a higher phosphotyrosine content of endosomal IR, which coincided with a more prolonged presence of IR in hepatic endosomes and a sustained endosomal recruitment of the endogenous molecular adaptor GRB14. Prior to organelle acidification, endosomal proteolysis of [Arg^{A0}]-HI yielded HI in a bestatin-sensitive manner whereas [Arg^{B31}-Arg^{B32}]-HI processing was not detected. Thus, internalised [Arg^{A0}]-HI may follow a specific proteolytic activating pathway which operates at an early stage of endocytosis and extends the IR signalling. Hence, based on the amount of proinsulin intermediates circulating in the blood, which account for 10–30% of insulin immunoreactivity in the fasting state [1, 32], and in the light of the in vivo effects of arginyl-insulins on hepatic IR signalling (this study), it may be hypothesised that arginyl-insulins fully participate in the insulinic action in hepatic target tissue.

The influence of endosomal proteolysis of insulin on IR trafficking and signal transduction has been previously inferred from a comparison of IR internalisation in liver parenchyma after in vivo challenge with receptor-saturating doses of insulin, high-affinity insulin analogues [14, 24, 26] or proinsulin [6]. While insulin was subject to rapid endosomal ligand dissociation and degradation [16, 19, 33], reduced in vivo and cell-free endosomal processing was observed with the H2-analogue [14, 24, 26] and proinsulin [6]. An altered IR phosphotyrosine profile was also observed at the endosomal locus, with this process being higher (H2-analogue) and of longer duration (H2-analogue and proinsulin) [6, 14, 24]. Using [Arg^{A0}]-HI as a ligand, an increase in the phosphorylation state of endosomal IR was observed which resembled that of the IR in response to the high-affinity H2-analogue [14, 24]. Moreover, an increase in IR transit through endosomes was observed with [Arg^{A0}]-HI, which may originate from: (1) the conversion of [Arg^{A0}]-HI into HI, which may delay the dissociation of insulin peptides from the endosomal IR and its subsequent recycling; (2) a reduced dissociation of [Arg^{A0}]-HI-receptor complex at the fluctuating endosomal pH compared with HI-receptor complex; and (3) a serum half-life of [Arg^{A0}]-HI longer than that of HI. Interestingly, as previously reported for the protease-resistant H2-analogue [15, 24], [Arg^{A0}]-HI induced an increase in the kinetics of MAP kinase activation and a more sustained association of GRB14 with the hepatic endosomes.

To test whether endosomal processing of [Arg^{A0}]-HI may influence IR trafficking and signalling at the endosomal locus, a detailed proteolysis study of arginyl-insulins was undertaken using a soluble endosomal lysate and RP-HPLC coupled to mass spectrometry analyses. In liver parenchyma the endosomal degradation of internalised insulin is thought to occur after acidification of the endosomal lumen by the aspartic acid protease cathepsin D which hydrolyses HI at Phe^{B24}-Phe^{B25} and Phe^{B25}-Tyr^{B26} peptide bonds [16, 19, 26]. Consistent with our previous studies, we have concluded in the present work that the endosomal acidic proteolytic activity directed towards the arginyl-insulins was comparable with that of cathepsin D, as indicated by the following observations: (1) the inhibitor profile of the endosomal proteolytic activity was similar to that of endosomal acidic insulinase activity and cathepsin D [16]; (2) immunodepletion of cathepsin D from ENs led to a loss of arginyl-insulin-degrading activity; and (3) the arginyl-insulins were found to inhibit ^{125}I-labelled Tyr^{A14}-HI degradation by ENs, confirming that the arginyl-insulins and HI share a common binding site on cathepsin D. On the basis of IC_{50} values, competition studies revealed that mature insulin and arginyl-insulins displayed nearly equivalent affinity for the endosomal acidic insulinase (cathepsin D). Finally, RP-HPLC and mass spectrometry analyses of the degradation products generated from arginyl-insulins by endosomal acidic insulinase (cathepsin D) revealed a pattern of cleavage sites similar to those observed using authentic insulin [16, 26]. The data suggest that the altered endosomal tyrosine-phosphorylation state of the IR-β subunit observed after [Arg^{A0}]-HI treatment did not arise from qualitative differences of ligand processing at acidic pH.

Previous studies have shown that proteases active at neutral pH are present in endosomes and that endosomal vesicles degrade various internalised ligands prior to the acidification step [34, 35]. Thus, it has been proposed that the initial step in insulin degradation occurs within hepatic endosomes at neutral pH and involves IDE, a neutral metalloendopeptidase [29]. Comparably, an endosomal membrane glucagonase activity transforms glucagon into miniglucagon at pH 7 [21]. We have also recently shown that rat hepatic endosomes contain a luminal truncated furin that cleaves the Arg^{193}-Ser^{194} peptide bond in the connecting A–B region of internalised diphtheria toxin at neutral pH [22]. We have now extended these observations to [Arg^{A0}]-HI and suggest that proinsulin intermediates possessing flanking sequences such as basic residues may undergo endosomal processing via a sequential degradation pathway beginning early, prior to organelle acidification, and following later under acidic conditions.

Our present data clearly show that [Arg^{A0}]-HI is susceptible to hydrolysis by a neutral Arg-aminopeptidase present in hepatic endosomes. Under our experimental conditions, fully processed HI was the unique product formed by the action of a bestatin-sensitive metallo-aminopeptidase. Using an alternative approach in which hydrolysis of the N-terminal Arg-peptide bond was measured by the generation

of fluorescent product from the non-fluorescent substrate Arg-MCA, we have confirmed that Arg-aminopeptidase is endosomally active in rat liver. Nardilysin and AP-B, two Arg-convertases that exhibit multiple physiological functions, have been reported to be present and active in hepatocytes. Nardilysin, a metallopeptidase, preferentially cleaves Arg bonds within paired basic residues [36] while AP-B catalyses the cleavage of Arg at the N-terminus of peptides [13]. Using immunoblot analyses we showed that a small but detectable amount of AP-B was present in hepatic endosomes while nardilysin was absent from this compartment. We were unable to test directly the role of AP-B in the endosomal processing of internalised [Arg^{A0}]-HI since the anti-AP-B antibody does not immunoprecipitate the rat AP-B enzyme (results not shown). Clearly, further studies are required to elucidate fully the functional significance of endosomal AP-B. However, regardless of the role of AP-B in removing Arg from endosomal substrates, our results support the hypothesis that the conversion of [Arg^{A0}]-HI into bioactive HI extends the duration of IR occupancy and signalling at the endosomal locus.

No degradation products were observed when hepatic endosomes were incubated at neutral pH with [Arg^{31}-Arg^{32}]-HI under conditions where the trimming of Arg^{A0} from monoarginyl-insulin was observed. Thus, the removal of Arg from Arg-extended peptides within the endosomal compartment may be highly selective. The present observation agrees well with our previous studies on the endosomal proteolysis of internalised human proinsulin (HPI) that show that rat liver endosomes produce selective cleavages in the Glu^{33}-Lys^{64} C-peptide without apparent modification of arginyl-peptide bonds [6]. Previously, other studies have reported that Triton X-100 solubilised rat liver endosomes [4] and rat hepatoma Fao cells stably transfected with HPI [5] processed HPI to des-[31,32]-HPI without conversion into mature HI. However, fully processed insulin was identified after transfection of hepatoma cells with the gene encoding rat proinsulin [5]. It has, however, also been reported that mouse serum contains a carboxypeptidase activity, suggested to be carboxypeptidase-N or kininase-I, which converted [Arg^{31}-Arg^{32}]-HI to HI by sequentially removing Arg^{31} and Arg^{32} [37]. Thus, the circulating blood may be the physiological locus for the removal of C-terminal Arg residues from arginyl-insulins.

The present study suggests that, besides genetically engineered mutant insulin analogues [14, 24, 26], incompletely cleaved proinsulin intermediates (in particular Arg-extended insulins) as well as unprocessed proinsulin [6] may represent potential therapeutic tools to achieve further improvements in glycaemic control during diabetic disease. Moreover, our study has identified endosomal neutral Arg-aminopeptidase, which acts on internalised arginyl-insulin and modulates insulin signalling at the endosomal locus in conjonction with IDE and cathepsin D, and represents a potential therapeutic target.

Acknowledgements We thank P. H. Cameron (McGill University, Montreal, Canada) for reviewing the manuscript.

Duality of interest The authors declare that there is no duality of interest associated with this manuscript.

References

1. Steiner DF, James DE (1992) Cellular and molecular biology of the beta-cell. Diabetologia 35:S41–S48
2. Steiner DF (1998) The proprotein convertases. Curr Opin Chem Biol 2:31–39
3. Wroblewski VJ, Masnyk M, Kaiser RE (1993) Metabolism of des (64, 65)-human proinsulin in the rat. Evidence for the proteolytic processing to insulin. Diabetes 42:1407–1414
4. Brennan SO, Peach RJ (1991) The processing of human proinsulin and chicken proalbumin by rat hepatic vesicles suggests a convertase specific for X–Y–Arg–Arg or Arg–X–Y–Arg sequences. J Biol Chem 266:21504–21508
5. Vollenweider F, Irminger JC, Gross DJ, Villa-Komaroff L, Halban PA (1992) Processing of proinsulin by transfected hepatoma (FAO) cells. J Biol Chem 267:14629–14636
6. Desbuquois B, Chauvet G, Kouach M, Authier F (2003) Cell itinerary and metabolic fate of proinsulin in rat liver: in vivo and in vitro studies. Endocrinology 144:5308–5321
7. Zeuzem S, Stahl E, Jungmann E, Zoltobrocki M, Schöffling K, Caspary WF (1990) In vitro activity of biosynthetic human diarginylinsulin. Diabetologia 33:65–71
8. DeHaen C, Little SA, May JM, Williams RH (1978) Characterization of proinsulin–insulin intermediates in human plasma. J Clin Invest 62:727–737
9. Kemmler W, Peterson JD, Steiner DF (1971) Studies on the conversion of proinsulin to insulin. I. Conversion in vitro with trypsin and carboxypeptidase B. J Biol Chem 246:6786–6791
10. Weinert M, Kircher K, Brandenburg D, Zahn H (1971) Crystallized arginyl A insulin. Hoppe Seyler Z Physiol Chem 352:719–724
11. Sreekanth R, Pattabhi V, Rajan SS (2008) Structural interpretation of reduced insulin activity as seen in the crystal structure of human Arg-insulin. Biochimie 90:467–473
12. Sreekanth R, Pattabhi V, Rajan SS (2009) Metal induced structural changes observed in hexameric insulin. Int J Biol Macromol 44:29–36
13. Pham VL, Cadel MS, Gouzy-Darmon C et al (2007) Aminopeptidase B, a glucagon-processing enzyme: site directed mutagenesis of the Zn^{2+}-binding motif and molecular modelling. BMC Biochem 8:21
14. Authier F, Di Guglielmo GM, Danielsen GM, Bergeron JJM (1998) Uptake and metabolic fate of [His^{A8}, His^{B4}, Glu^{B10}, His^{B27}] insulin in rat liver in vivo. Biochem J 332:421–430
15. Desbuquois B, Béréziat V, Authier F, Girard J, Burnol AF (2008) Compartmentalization and in vivo insulin-induced translocation of the insulin-signaling inhibitor Grb14 in rat liver. FEBS J 275:4363–4377
16. Authier F, Métioui M, Fabrega S, Kouach M, Briand G (2002) Endosomal proteolysis of internalized insulin at the C-terminal region of the B chain by cathepsin D. J Biol Chem 277:9437–9446
17. Authier F, Mort JS, Bell AW, Posner BI, Bergeron JJM (1995) Proteolysis of glucagon within hepatic endosomes by

membrane-associated cathepsins B and D. J Biol Chem 270: 15798–15807
18. Authier F, Métioui M, Bell AW, Mort JS (1999) Negative regulation of epidermal growth factor signaling by selective proteolytic mechanisms in the endosome mediated by cathepsin B. J Biol Chem 274:33723–33731
19. Authier F, Rachubinski RA, Posner BI, Bergeron JJM (1994) Endosomal proteolysis of insulin by an acidic thiol metalloprotease unrelated to insulin-degrading enzyme. J Biol Chem 269:3010–3016
20. Authier F, Cameron PH, Taupin V (1996) Association of insulin-degrading enzyme with a 70 kDa cytosolic protein in hepatoma cells. Biochem J 319:149–158
21. Authier F, Cameron PH, Merlen C, Kouach M, Briand G (2003) Endosomal proteolysis of glucagon at neutral pH generates the bioactive degradation product miniglucagon-(19-29). Endocrinology 144:5353–5364
22. El Hage T, Decottignies P, Authier F (2008) Endosomal proteolysis of diphtheria toxin without toxin translocation into the cytosol of rat liver in vivo. FEBS J 275:1708–1722
23. Lowry OH, Rosebrough NJ, Farr AL, Randall RJ (1951) Protein measurement with the Folin phenol reagent. J Biol Chem 193:265–275
24. Authier F, Merlen C, Amessou M, Danielsen GM (2004) Use of high affinity insulin analogues to assess the functional relationships between insulin receptor trafficking, mitogenic signaling and mRNA expression in rat liver. Biochimie 86:157–166
25. Authier F, Janicot M, Lederer F, Desbuquois B (1990) Fate of injected glucagon taken up by rat liver in vivo. Degradation of internalized ligand in the endosomal compartment. Biochem J 272:703–712
26. Authier F, Danielsen GM, Kouach M, Briand G, Chauvet G (2001) Identification of insulin domains important for binding to and degradation by endosomal acidic insulinase. Endocrinology 142:276–289
27. Authier F, Kouach M, Briand G (2005) Endosomal proteolysis of insulin-like growth factor-I at its C-terminal D-domain by cathepsin B. FEBS Lett 579:4309–4316
28. Hwang SR, O'Neill A, Bark S, Foulon T, Hook V (2007) Secretory vesicle aminopeptidase B related to neuropeptide processing: molecular identification and subcellular localization to enkephalin- and NPY-containing chromaffin granules. J Neurochem 100:1340–1350
29. Hamel FG, Mahoney MJ, Duckworth WC (1991) Degradation of intraendosomal insulin by insulin-degrading enzyme without acidification. Diabetes 40:436–443
30. Wouters S, Leruth M, Decroly E et al (1998) Furin and proprotein convertase 7 (PC7)/lymphoma PC endogenously expressed in rat liver can be resolved into distinct post-Golgi compartments. Biochem J 336:311–316
31. Fontès G, Lajoix AD, Bergeron F et al (2005) Miniglucagon (MG)-generating endopeptidase, which processes glucagon into MG, is composed of N-arginine dibasic convertase and aminopeptidase B. Endocrinology 146:702–712
32. Halban PA (1992) Proinsulin processing in the regulated and the constitutive secretory pathway. Diabetologia 37:S65–S72
33. Desbuquois B, Janicot M, Dupuis A (1990) Degradation of insulin in isolated liver endosomes is functionally linked to ATP-dependent endosomal acidification. Eur J Biochem 193:501–512
34. Berg T, GjØen T, Bakke O (1995) Physiological functions of endosomal proteolysis. Biochem J 307:313–326
35. Authier F, Posner BI, Bergeron JJM (1996) Endosomal proteolysis of internalized proteins. FEBS Lett 389:55–60
36. Chow KM, Oakley O, Goodman J et al (2003) Nardilysin cleaves peptides at monobasic sites. Biochemistry 42:2239–2244
37. Isaac RE, Michaud A, Keen JN et al (1999) Hydrolysis by somatic angiotensin-I converting enzyme of basic dipeptides from a cholecystokinin/gastrin and a LH-RH peptide extended at the C-terminus with Gly-Arg/Lys-Arg, but not from diarginyl insulin. Eur J Biochem 262:569–574